Least-squares wave-equation migration for AVP/AVA inversion

Henning Kuehl and Mauricio D. Sacchi - Department of Physics, University of Alberta

CSEG Geophysics 2002

Abstract

Wave-equation migration is known for its ability to generate accurate structural images in complex geological settings. Recently, imaging principles have been developed that allow for the extraction of amplitude variations as a function of offset ray-parameter or angle (AVP or AVA) from the downward continued wavefield. We propose the least-squares (LS) approach to wave-equation migration in order to generate high quality ray parameter common image gathers (CIGs). As we have previously demonstrated with the Marmousi model, least-squares imaging with a smoothing constraint on the ray parameter CIGs can mitigate kinematic artifacts. In this paper we study the effect of the smoothing regularization for incomplete and noisy data in more detail. Relatively simple examples based on the full wave-equation allow us to better assess the performance and appropriateness of the LS smoothing regularization in terms of AVP/AVA preservation. The results are promising and suggest that least-squares migration, although computationally expensive, holds benefits for producing high quality AVP/AVA estimates.

Introduction

In recent years, increasing attention has been given to wave-equation migration imaging principles that attempt to yield information about amplitude variations with offset ray parameter (AVP) or reflection angle (AVA) (e.g., Stolt and Weglein , 1985; de Bruin et al., 1990; Prucha et al., 1999; Wapenaar et al., 1999, Mosher and Foster, 2000; Sava et al., 2001). In this paper we focus on the ray parameter imaging principle as described, for instance, in Sava et al. (2001). As opposed to migration in the τ-p domain (Ottolini and Claerbout, 1984), the ray parameter imaging principle extracts constant (half)offset ray-parameter gathers from the downward continued wavefield thereby relaxing the restriction to horizontally layered media. We combine extended double-square-root (DSR) propagators (e.g., Clayton and Stolt, 1981; Gazdag and Sguazzero, 1984 and Stoffa et al., 1990) with the ray parameter imaging technique in a least-squares (LS) optimization algorithm with a smoothness constraint on the ray parameter common image gathers (CIGs). This idea is similar to the work done by Duquet et al. (2000) who exploited the smoothing constraint to mitigate migration artifacts in Kirchhoff migration. However, it is important to further investigate how truthfully the constrained LS migration estimates the AVP function and how the noise and missing data affect the inversion result.

Method

We employ modeling and migration wave-equation operators to invert the linear system:

$$d(y, h, \omega) = \mathbf{L}\, m(y, p, z) + n, \tag{1}$$

where *d* is the binned and usually incompletely sampled seismic wavefield data. The data are given in midpoint coordinate *y*, (half)offset *h* and temporal frequency ω. The term *n* represents additive noise. The model function *m* contains the (half)offset ray parameter *p* dependent CIGs at the midpoint position *y* and depth *z*. The modeling operator **L** is a combination of the adjoint of the ray parameter imaging operator described in Sava et al. (2001) and the double-square-root (DSR) upward wavefield propagator. Depending on the complexity of the underlying migration velocity field the DSR propagator is extended by a split-step operator and can also be applied in a multiple-reference-velocity mode (Gazdag and Sguazzero, 1984; Stoffa et al., 1990). The following cost function is iteratively minimized by a conjugate gradient (CG) algorithm:

$$F(m) = \left\| \mathbf{W} \left(d(y, h, \omega) - \mathbf{L}\, m(y, p, z) \right) \right\|^2 + \lambda^2 \left\| \partial_h m(y, h, z) \right\|^2 , \tag{2}$$

where **W** is a diagonal weighting operator with zero weights for dead traces and non-zero weights for live traces. The CG minimization amounts to an iterative application of the adjoint migration operator **L'** and the modeling operator **L**. Besides the data-misfit term, we have added a regularization term that penalizes "roughness" along the ray-parameter *p*. "Roughness" is attributed to missing data, noise and numerical operator artifacts. The tradeoff parameter λ determines the amount of smoothing. This regularization approach has proven successful in a kinematic sense when applied to the Marmousi data set (Kuehl and Sacchi, 2001).

The inverted ray parameter gathers *m* can be converted to AVA plots by means of the relationship:

$$\theta = \arcsin \left(\frac{vp}{2 \cos \phi} \right), \tag{3}$$

where θ is the incidence angle on a locally plane reflector element, *v* is the migration velocity directly above the reflector and ϕ is the local reflector dip. If only the migration operator $\mathbf{L}'$ is to be applied the AVA can be improved by scaling the amplitudes with the factor $C = \frac{2 \cos \theta}{c(z)}$. This factor was introduced for horizontally layered media by Wapenaar et al. (1999). Sava et al. (2001) also derived this scaling factor within the framework of least-squares migration to approximate the least-squares solution. The factor C removes the tendency of the migration operator $\mathbf{L}'$ to overestimate the AVA for large angles.

Example

We generated an acoustic finite difference data set based on a horizontally layered model. The model parameters in terms of compressional wave velocity, density and layer thickness are listed in Table 1. Except for the geometry, the medium properties are the same as in the acoustic example of de Bruin et al. (1990). The data consist of 100 midpoints with 50 offsets ranging in half-offset h from 0 to 980 m. Table 1 also contains the maximum reflection angles for the given offset range. To test the effect of dead data traces 50% of the data were randomly set to zero (Figure 1). The migrated ray parameter CIG of the incomplete data is shown in Figure 2A. The missing data caused spurious energy and discontinuities in the CIG. For better assessment of the quality of the CIG we picked the AVP of the four reflectors. To mitigate the discontinuities ("roughness") introduced by finite aperture artifacts and missing data a six point moving average filter (equivalent to a ray parameter range of 0.096 s/km) was applied to the AVP curves. The curves were then converted to their AVA equivalents with equation (3). Furthermore, we scaled the AVA amplitudes by the weighting factor C. The AVA curves in Figure 3A exhibit rapid amplitude changes and deviate strongly from the theoretical AVA. Since no transmission loss affects the first reflection, all four curves were scaled by trying to match the first reflector to the theoretical values. The deeper reflectors are increasingly underestimated due to unaccounted for transmission losses. The LS migration (18 CG iterations) with ray parameter smoothing has retrieved a continuous and cleaner CIG (Figure 2B). Finite aperture effects are mitigated. The corresponding picked and converted AVA is depicted in Figure 3B. Despite inevitable finite aperture effects the inverted AVA matches the theoretical AVA well within the retrievable angle range. To test the influence of the data weighting operator **W** on the inversion result we ran the same example without data weighting. The inverted CIG is shown in Figure 2C. Not all of the spurious energy could be suppressed. Furthermore, the picked AVA exhibits undulations that are due to the missing data traces (Figure 3C). This example demonstrates that smoothing along the ray parameter alone can only mitigate kinematic artifacts at best. If reliable AVA estimates are desired care must be taken to discard unreliable or dead traces from the inversion.

Table 1: Model parameters.

	c (m/s)	ρ (g/cm^3)	Thickness (m)	Max. angle (degrees)
Layer 1:	**2000**	**2.0**	**800**	**51**
Layer 2:	**2500**	**2.5**	**300**	**48**
Layer 3:	**2000**	**1.5**	**500**	**29**
Layer 4:	**2000**	**2.25**	**400**	**25**
Half-space:	**2500**	**1.4**		

Conclusions

Wave-equation migration using a ray parameter imaging principle allows for the generation of half-offset ray parameter CIGs. If cast into the least-squares migration framework, ray parameter imaging with a ray parameter dependent smoothing constraint helps to generate high quality CIGs. The logic behind ray parameter smoothing is based on the notion that rapid amplitude changes or discontinuities along the ray parameter axis stem from numerical imaging artifacts and missing data, not AVA effects. Using acoustic finite difference data based on a stratified subsurface it is found that LS wave-equation migration can retrieve AVA functions that, despite inevitable finite aperture effects, are close to the true AVA. The smoothness constraint proves especially beneficial when the seismic data are compromised by incompleteness. Acquisition footprint effects in terms of kinematic artifacts and amplitude distortion in the ray parameter CIGs are successfully mitigated. However, further tests have to show how well LS wave-equation migration with ray parameter smoothing can produce reliable true amplitude AVP/AVA estimates in complex media.

Acknowledgements

This work has been funded by PanCanadian, Geo-X, Schlumberger Foundation, Veritas Geoservices, NSERC and Alberta Energy Research Instittiute. We are grateful for their support.

References

Clayton, R.W., and Stolt, R.H., 1981, A Born-WKBJ inversion method for acoustic reflection data: Geophysics, **46**, 1559-1567.

De Bruin, C.G.M., Wapenaar, C. P.A., and Berkhout, A.J., 1990, Angle dependent reflectivity by means of prestack migration: Geophysics, **55,** 1223-1234.

Duquet, B., Marfurt, J.K., and Dellinger, J.A., 2000, Kirchhoff modeling, inversion for reflectivity, and subsurface illumination: Geophysics, **65**, 1195-1209.

Gazdag, J., and Sguazzero, P., 1984, Migration of seismic data by phase shift plus interpolation: Geophysics, **49**, 124-131.

Kuehl, H., and Sacchi, M.D., 2001, Generalized least-squares DSR migration using a common angle imaging condition, 71st Ann. Internat. Mtg., Soc. Expl. Geophys., Expanded Abstracts, MIG 4.4.

Mosher, C.C., and Foster, D.J., 2000, Common angle imaging conditions for pre-stack depth migration, 70th Annual Internat. Mtg., Soc. Expl. Geophys., Expanded Abstracts, MIG 4.4.

Ottolini, R., and Claerbout, J.F., 1984, The migration of common midpoint slant stacks: Geophysics, **49**, 237-249.

Prucha, M., Biondi, B., and Symes, W., 1999, Angle-domain common image gathers by wave equation migration, 69th Ann. Internat. Mtg., Soc. Expl. Geophys., Expanded Abstracts, 824-827.

Sava, P., Biondi, B., and Fomel, S., 2001, Amplitude preserved common image gathers by wave-equation migration, 71st Ann. Internat. Mtg., Soc. Expl. Geophys., Expanded Abstracts, AVO 5.3.

Stoffa, P.L., Fokkema, J.T.. de Luna Freire, R.M., and Kessinger, W.P., 1990, Split-step migration: Geophysics, **55,** 410-421.

Stolt, R. H., and Weglein, A. B., 1985, Migration and inversion of seismic data: Geophysics, **50**, 2458-2472.

Wapenaar, C. P. A., van Wijngaarden, A.-J., van Geloven, W., and van der Leij, T., 1999, Apparent AVA effects of fine layering: Geophysics, **64**, 1939-1948.

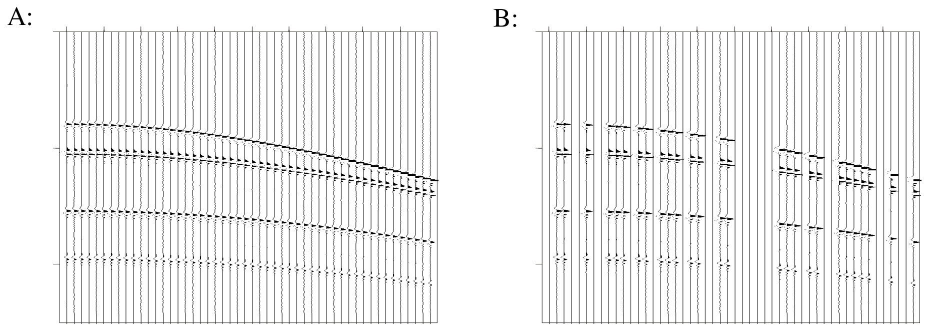

Figure 1: CMP data before (A) and after (B) randomly removing 50% of the data.

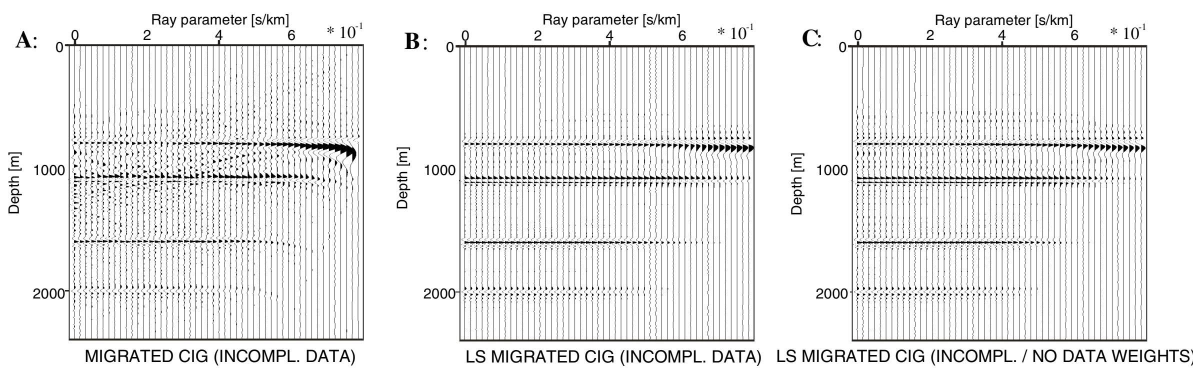

Figure 2: Ray parameter CIGs of the incomplete data after migration (A), LS migration (B), and LS migration without data weighting (C).

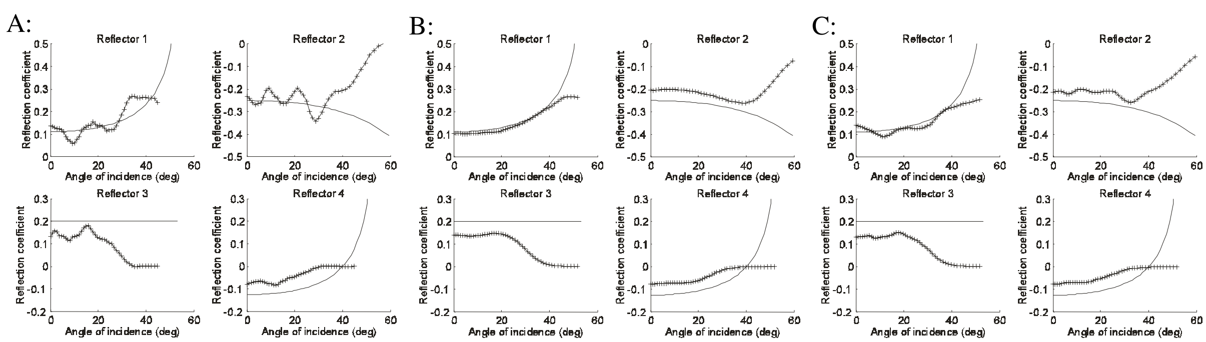

Figure 3: A: Picked AVA from the CIG in Figure 2A. The solid lines indicate the true AVA in an acoustic medium. A moving average filter and a scaling factor (see text) has been applied to the AVA. B: Picked AVA from the CIG in Figure 2B. No additional averaging or scaling has been applied to the AVA.C: Picked AVA from the CIG in Figure 2C. The disabled data weighting has caused the LS solution to be biased by the missing data.